ACS SENSORS

Open Access
This article is licensed under CC-BY 4.0

pubs.acs.org/acssensors
Article

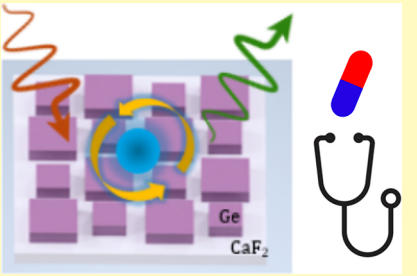
Metasurface-Enhanced Infrared Spectroscopy for Quantitative Molecular Sensing: A Proof-of-Concept Study for Therapeutic Drug Monitoring

Kezheng Li,* Pin Dong, Aneesh Vincent Veluthandath, Soheila Kharratian, Augusto Martins, Ganapathy Senthil Murugan, Yue Wang,* and Thomas F. Krauss

Cite This: *ACS Sens.* 2026, 11, 8387−8394
Read Online

ACCESS | Metrics & More | Article Recommendations | Supporting Information

ABSTRACT: Therapeutic drug monitoring (TDM) is the clinical practice of measuring specific drugs at designated intervals to maintain a constant concentration in a patient's bloodstream. However, detecting clinically relevant levels (typically in the μg/ml range) remains challenging outside the laboratory, as current analytical methods use elaborate sample preparation protocols and complicated measurement procedures. Here, we present a metasurface-assisted Fourier-transform infrared approach using dried samples that enhances molecular absorption by aligning their vibrational modes with the metasurface resonance; the metasurface supports a guided-mode resonance that hybridizes with the vibrational frequency of the drug molecule, thereby increasing the effective absorbance significantly. The metasurface topology also promotes ordered drug crystallization in regions with the strongest light−matter interaction, further contributing to the absorption enhancement. Using this design, we are able to consistently detect phenytoin in serum below the therapeutic range of 10–20 μg/ml by achieving a limit of detection of 1.4 μg/ml, which is limited by the drying process. This proof of concept for TDM at concentrations in the sub-clinical level highlights the significant potential for metasurface-enhanced spectroscopy and offers a path toward compact, high-performance infrared sensors for healthcare applications.



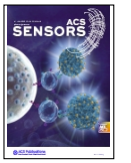
KEYWORDS: *metasurfaces, surface-enhanced infrared absorption (SEIR), therapeutic drug monitoring (TDM), infrared spectroscopy, point-of-care biosensors, phenytoin*

Therapeutic drug monitoring (TDM) is a branch of clinical analytical chemistry and clinical pharmacology that specializes in the measurement of medication levels in blood. The main focus of TDM is on drugs with a narrow therapeutic range, i.e., drugs that can easily be underdosed or overdosed.[1] For example, phenytoin is an antiepileptic drug with a therapeutic range between 10 and 20 μg/ml, whereby concentrations below 10 μg/ml may be ineffective while concentrations above 20 μg/ml can lead to toxicity.[2] Accurate and rapid quantification of drug concentration at these levels within a patient's bloodstream is therefore critical for effective treatment. Phenytoin TDM is a well-established, guideline-recommended clinical practice owing to its narrow therapeutic window and nonlinear pharmacokinetics[25] and is currently performed at the bedside using automated immunoassays (e.g., fluorescence polarization immunoassays (FPIA) and enzyme multiplied immunoassay technique (EMIT)).[26,27]

Chromatographic methods, such as liquid chromatography–tandem mass spectrometry (LCMS) or the enzyme-linked immunosorbent assay (ELISA),[3] instead serve as reference and confirmatory methods for TDM, offering higher analytical specificity; however, their confinement to laboratory settings, i.e., expensive instrumentation and the need for skilled personnel, leads to a long turnaround time.[4] All of these factors prevent real-time or point-of-care monitoring; indeed, point-of-care implementation of phenytoin TDM, in particular, remains limited, driven more by translational and validation barriers than by a lack of sensing technologies.[28] While electrochemical sensors have been explored as alternatives,[5] they suffer from drift, electrode fouling, and poor reproducibility, which limit their reliability for long-term monitoring.

In contrast, benchtop Fourier-transform infrared (FTIR) spectroscopy offers a truly label-free and on-site analytical alternative. FTIR provides molecular fingerprint information, enabling high specificity for identifying relevant drug molecules. However, especially for blood or serum samples, the strong water absorption and overlapping protein bands often obscure weak drug signals, complicating direct detection and quantification. The attenuated total reflectance (ATR) FTIR configuration conducted on dried samples partially addresses this

Received: May 22, 2026
Revised: August 13, 2026
Accepted: August 14, 2026
Published: August 25, 2026



Downloaded from pubs.acs.org/ascefj/article-pdf/11/9/8387/6739458/se-2026-022393.pdf by guest on 04 November 2026

© 2026 The Authors. Published by American Chemical Society

https://doi.org/10.1021/acssensors.6c02239
ACS Sens. 2026, 11, 8387−8394

challenge by extending the effective interaction path length through evanescent field coupling, improving the sensitivity over conventional transmission or reflection setups. Nevertheless, even ATR-FTIR typically lacks the sensitivity required to detect drug concentrations in the required low μg/ml range essential for TDM.

More advanced optical methods, such as polarization-modulated infrared reflection–absorption spectroscopy (PM-IRRAS),[6] can further improve the detection limit by suppressing the background absorption using a polarization-based differential measurement, which results in an enhanced signal-to-noise ratio. However, PM-IRRAS relies on grazing-incidence optics with a single-pass absorption geometry and is limited to probing surface-confined or monolayer species, which is inadequate for bulk biological samples such as serum or blood. Therefore, it is not suitable for routine or bedside monitoring applications.

Overall, the primary limitation of these methods is their insufficient sensitivity. To address this limitation, the sensitivity can be significantly enhanced by strengthening the light–matter interactions via approaches such as surface-enhanced Raman spectroscopy (SERS) or surface-enhanced infrared absorption spectroscopy (SEIRA).[7−11] For example, SEIRA samples usually exploit a localized field, which can enhance molecular absorption by coupling and hybridizing photonic resonances with molecular vibrational modes. When the vibrational mode of a molecule is coherently coupled to the resonant mode of a photonic structure, the light–matter interaction is significantly amplified, leading to enhanced absorption effects that are measurable as resonance dips. To evaluate the performance of such structures, a practical figure of merit (FOM) is the absorption enhancement, which quantifies how much the molecular absorptance is amplified. This FOM inherently reflects the effects of local field enhancement, mode overlap, the resonance's quality factor Q, and effective interaction volume and coupling efficiency, making it a direct metric for comparison. For example, Adato and Altug[9] have demonstrated a plasmonic antenna to enhance the absorption of a protein monolayer 10-fold compared to IRRAS-FTIR. Tittl and co-workers[7] reported that quasi-bound state in the continuum (quasi-BIC) dielectric metasurfaces achieved more than one order-of-magnitude enhancement in molecular absorption for physiosorbed monolayers, relative to IRRAS. Using a comparable geometry, Leitis et al.[10] further exploited angular sensitivity to demonstrate a 50-fold enhancement in the absorption of poly(methyl methacrylate) (PMMA) thin films compared with IRRAS, while Kharratian et al.[11] showed that dielectric nanohole arrays achieve more than an order-of-magnitude enhancement in molecular absorption in solution relative to ATR-FTIR. Numerous other studies have also been reported without specifying exact absorption enhancement factors,[9,12] yet they clearly demonstrate the growing attention in this field. These examples illustrate the potential of resonantly enhanced mid-IR spectroscopy to detect low concentrations of molecules. Nevertheless, none of these structures have yet been applied to the important problem of TDM. For bedside TDM, several practical requirements must be met: the enhancement should extend over a large fraction of the sensing area rather than being confined to sparse, nanoscale hotspots with limited filling factors, so that the measured signal is robust to spatially nonuniform analyte distribution across a macroscopic FTIR beam spot; and the system must be tolerant to angle and alignment variations while enabling rapid measurement and short sample turnaround times. Existing SERS and SEIRA platforms do not simultaneously satisfy all of these requirements.[22−24]

Since compact FTIR systems are already being used in research and pharmaceutical settings,[13] and are beginning to find applications in clinical environments,[14] we propose a new dielectric metasurface design that can be readily integrated with compact FTIR systems to enhance sensitivity and improve the limit of detection (LoD). The key novelty in our approach is the choice of an angle-tolerant metasurface design, which is essential for ensuring compatibility with the focused beam of an FTIR system. Our approach offers the real possibility of moving TDM from the laboratory to the bedside. As a proof of concept, we target phenytoin (PHT), a widely prescribed antiepileptic drug, and show that we are able to detect sub-clinically relevant concentrations. The sub-clinical concentration we demonstrate allows us to accommodate the tolerances and reproducibility issues of a system that may actually be used in clinical practice.

■ DESIGN AND RESULTS

Our metasurface consists of a patterned 400 nm thick germanium (Ge) layer on a bulk calcium fluoride (CaF_2) substrate. It is designed to operate in the spectral range of 5–9 μm (Figure S1, Section 1 in Supplementary Information) and is illustrated in Figure 1a. The periodical structure is a two-dimensional array of a tetramer unit cell that supports a guided mode resonance. The design is inspired by the BIC phenomenon with intentionally broken symmetry to allow coupling to the guided mode.[15] When this resonance mode is tuned to coincide with the molecular vibrational mode in wavelength, the two modes hybridize, which enhances the light-matter interaction and amplifies molecular absorption.[16] This results in a pronounced absorption dip in the reflection spectrum of the sample (Figure 1e).

The geometric parameters of our metasurface (see Figure 1b) are chosen by considering both the resonance amplitude and the Q factor[17] while tuning the resonance to the target wavelength (see Figure 1d, and full details are provided in Figure S2, Section 2 in the Supporting Information). With $a = 2$ μm, $b = 1.5$ μm, $w = 1$ μm, and the period of 5.4 μm, the structure supports a mode aligned with the absorption peak of phenytoin (PHT) at 5.62 μm (1778 cm^{-1}) as shown in the simulated reflectance spectrum in Figure 1d. Notably, PHT has two characteristic absorption peaks: 5.62 μm (1778 cm^{-1}) and 5.78 μm (1728 cm^{-1}). Since the 5.78 μm peak overlaps with serum protein absorption bands (details are provided in Figure S3, Section 3, Supporting Information), the 5.62 μm peak is selected as the target peak for TDM. Figure 1c presents a simulated top view of the electrical-field intensity distribution at the middle height of the structure. The field intensity distribution shows that the strongest field enhancement occurs at the corners of the tetramers and gradually merges into the gap regions. This suggests that if the drug molecules crystallize in the gaps, they will strongly overlap with the localized field, promoting optical absorption. The simulation of a phenytoin thin film on top of the metasurface, see Figure 1f, shows that absorption-induced dip area has good tolerance to the incident angle, which is better than that of a simple periodic array[11] and compatible with the half-angle of the FTIR thermal source that we use (more details are provided in Section 10 in the Supporting Information).

Downloaded from pubs.acs.org/asceff/article-pdf/11/9/8387/6739358/se-2026-022393.pdf by guest on 04 November 2026

https://doi.org/10.1021/acssensors.6c02239
ACS Sens. 2026, 11, 8387−8394

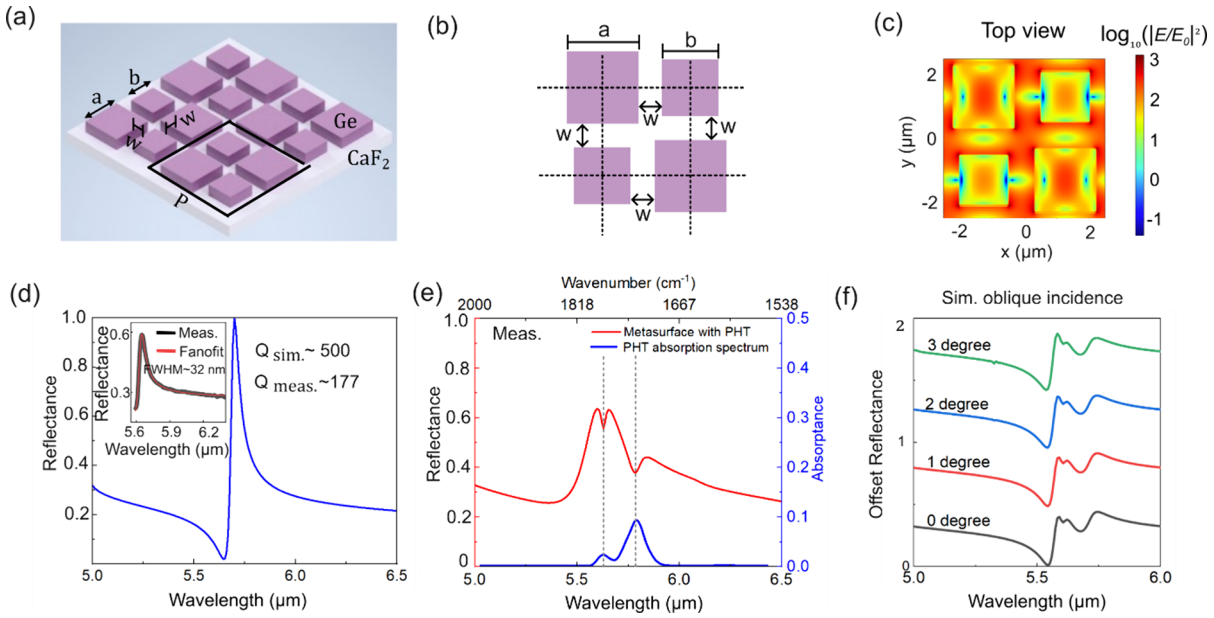


Figure 1. Design of the metasurface and mechanism of molecular absorption enhancement. (a) Schematics of the three-dimensional and (b) two-dimensional unit-cell geometry (top view) of the metasurface. The black solid lines in (a) mark the unit-cell boundaries, consisting of four asymmetric germanium square prisms in Ge on a CaF_2 substrate. The broken symmetry enables the excitation of a guided mode with a high-quality factor even under noncollimated illumination. (c) Simulated electric-field distribution at the half-height plane of the structure, showing strong field confinement in the corner of the tetramers. $|E_0|$ denotes the incident field amplitude. The measured Q factor is 177, compared to the simulated value of 500 for plane-wave illumination, as shown in (d) and the inset. (e) The blue curve is the absorption spectrum of 1 mg/ml of PHT in dried condition measured by ATR-FTIR. The red curve is the measured reflection spectrum with dried phenytoin layer (PHT) on the metasurface. The gray dashed lines indicate that the PHT absorption bands align with the resonance dips. (f) Simulated reflection spectra (with offset) of the metasurface coated with a 1 μm-thick PHT layer, for incidence angles varying from 0° to 3°. The variation of the dip area changes within 7% between 0° and 3° tilt of the incident beam.

Figure 2 illustrates the fabricated metasurface. The SEM micrographs in Figure 2b,c show the unit cell size of 5.4 μm, with $w \approx 1$ μm gaps between adjacent squares. For the measurement, samples were prepared in a dried state to eliminate background interference from water. To study the molecular loading, SEM micrographs of the dried PHT solution (in ethyl acetate) are shown in Figure 2e,f, revealing that PHT molecules accumulate and crystallize within the grooves of the structures around the region where the E-field enhancement is strongest. This accumulation ensures a good spatial overlap with the optical mode in addition to the spectral overlap between the resonance and the molecular absorption line, which together yield significant absorption enhancement. For comparison, a PHT droplet dried on a flat Ge substrate forms random shapes (Figure 2d showing the edge of the coffee ring). A SEM micrograph with a larger field of view comparing PHT dried on flat Ge and on a metasurface is shown in Figure S4 (Section 4, Supporting Information).

To experimentally validate the enhancement, we built an open-path reflection unit, shown in Figure 3, which is inserted into a commercial FTIR spectrometer. This arrangement allows us to measure both the metasurface resonance and the enhanced molecular absorption spectrum (detailed descriptions are in the Methods section). In order to quantify the enhancement factor over ATR-FTIR, we compare the LoDs of a PHT-spiked serum sample between the two methods.

Starting with ATR-FTIR measurements, PHT was spiked into the processed serum sample using our recently developed protocol[19] with concentrations of 50, 100, and 150 μg/ml. We deposited 10 μl of each solution and dried on the ATR sensor surface (applying excessive volume, e.g., >10 μl, would cause overflow of the ATR sensing area, resulting in nonreproducible measurements, as shown in Figure S5, Section 5, Supporting Information). The corresponding absorption spectra are presented in Figure 4b, where the gray arrow marks the target absorption peak at 5.62 μm, while the purple curve represents the spectrum measured without PHT sample in air. From the graph, the LoD was determined by the concentration that is equal to three times the standard deviation ($3\sigma = 0.00175$). While the dried PHT sample with the concentration of 150 μg/ml is clearly distinguishable, the 100 μg/ml sample exhibits a signal slightly above the 3σ threshold, shown by the black dashed line, and the signal for the 50 μg/ml sample remains within the noise level. Hence, the LoD of the ATR-FITR for dried PHT-serum is estimated to be approximately 100 μg/ml.

For the metasurface-based measurements, the sensing area is approximately 30 times larger than that of the ATR sensor; therefore, 300 μl of serum was used to ensure an equivalent molecular coverage per unit area. Besides, this volume provides sufficient surface coverage, strong absorption signals, and relatively short evaporation time. Details are also available in Sections 5 and 6, Supporting Information. The serum samples were processed using the same protocol described previously.[19] Briefly, the procedure involves three steps: removal of lipids, removal of small water-soluble molecules, and isolation of proteins. After processing, PHT was spiked into the samples at different concentrations. We discuss the reason for this sample

Downloaded from pubs.acs.org/acsecf/article-pdf/11/9/8387/6739458/se-2026-022393.pdf by guest on 04 November 2026

https://doi.org/10.1021/acssensors.6c02239
ACS Sens. 2026, 11, 8387−8394

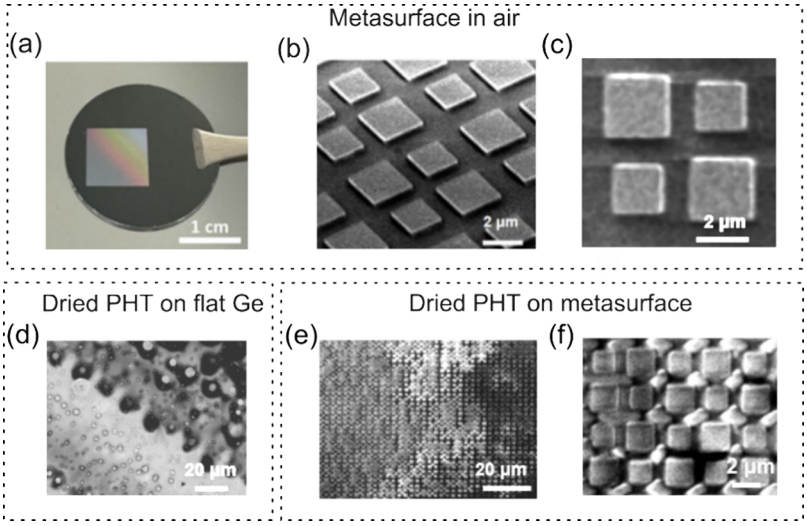


Figure 2. Fabricated metasurface and dried PHT sample. (a) Photograph of the fabricated metasurface. (b) SEM micrograph of the metasurface as fabricated, and (c) top view of one unit cell. (d) SEM micrograph of the dried PHT on a flat Ge surface and (e and f) the metasurface after PHT crystallization, showing the PHT molecules accumulating in the corners and grooves of the metasurface.

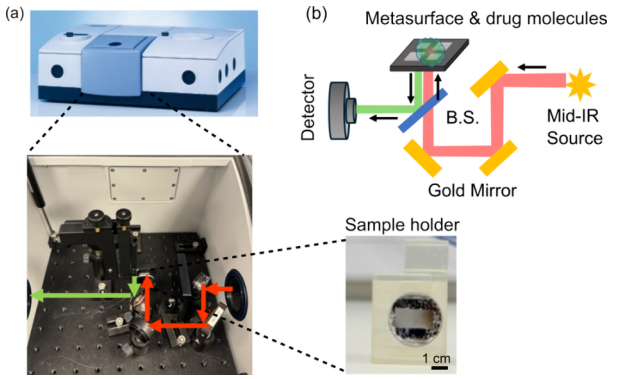


Figure 3. Metasurface implementation in a commercial FTIR spectrometer. (a) Experimental setup with the metasurface integrated into a commercial FTIR system using a custom open-path reflection unit. The unit consists of a mid-IR beamsplitter, gold mirrors, and a 3D printed sample holder for positioning the metasurface, as schematically shown in (b).

preparation strategy and its equivalence to alternative clinical workflows in the Discussion section. Figure 4a shows the PHT solution dried on the metasurface, exhibiting a characteristic coffee-ring effect. Reflection spectra were collected at room temperature under compressed air purged conditions, with measurements taken at ten different locations on each sample to average out nonuniformities caused by drying. The enhanced absorption is quantified by integrating the area between the resonance dip and the refractive-index-matched reference profile, as highlighted in yellow in Figure 4h. Together, they demonstrate that our method is indeed capable of detecting very low concentrations of PHT in serum. Figure 4c shows a range of concentrations between 0 and 5 μg/ml, with Figure 4d–g highlighting the spectra for each specific value. Concentrations below 0.1 μg/ml can be clearly observed, with 0.01 μg/ml detectable just beyond the noise. Figure 4i summarizes the response against concentration based on the error bars which represent the standard deviation of the dip area from multiple measurements across repeated dry–wash cycles. From Figure 4i, a realistic LoD for repeatable measurements using the commonly accepted laboratory rule (defined as three times the standard deviation divided by the slope) results in an LoD of 1.4 μg/ml, which is 10-fold lower than the clinical requirement. For comparison, without the metasurface, the PHT absorption dip cannot be distinguished at all in the reflection measurements. For example, a measurement on a flat Ge-on-CaF_2 substrate with 300 μl of 100 μg/ml PHT-spiked serum shows no discernible feature, as presented in Figure S7 in the Supporting Information. Note that our LoD is calculated based on four repeats of measurements. Further comparison between the LoD of the metasurface and ATR approach is shown in Section 11 in Supporting Information.

■ DISCUSSION AND CONCLUSION

We have demonstrated a metasurface-based SEIRA approach that could be potentially useful for bedside therapeutic drug monitoring. We are able to repeatably detect dried serum with a model drug, phenytoin, at 1.4 μg/ml. This result is significantly improved compared to other mid-IR spectroscopic techniques; for example, the LoD of dried PHT-serum sample for ATR-FTIR is 100 μg/ml and for IRRAS-FTIR, the LoD is 5 μg/ml.[19] It is also interesting to compare our results to the related technique of SERS, which does not suffer from water absorption and for which an excellent result of 1.8 μg/ml[20] was reported. We note, however, that SERS is known to suffer from quantification issues as minute changes in molecular distribution may change the overlap with the nanoscale hotspots that SERS exploits; our resonant mode is much larger in comparison. Regarding related metasurface work, we note that previous studies have focused on strong absorbers or neat analytes,[18] which are considerably easier to detect than the weakly absorbing, clinically relevant drug molecules. Therefore, our approach is able to tackle the much more difficult problem of detecting low concentrations of drug molecules in a serum sample. We explain this improvement with the combination of a relatively high Q-factor, the strong overlap between the resonant mode

Downloaded from pubs.acs.org/ascefj/article-pdf/11/9/8387/6739358/se-2026-022393.pdf by guest on 04 November 2026

https://doi.org/10.1021/acssensors.6c02239
ACS Sens. 2026, 11, 8387−8394

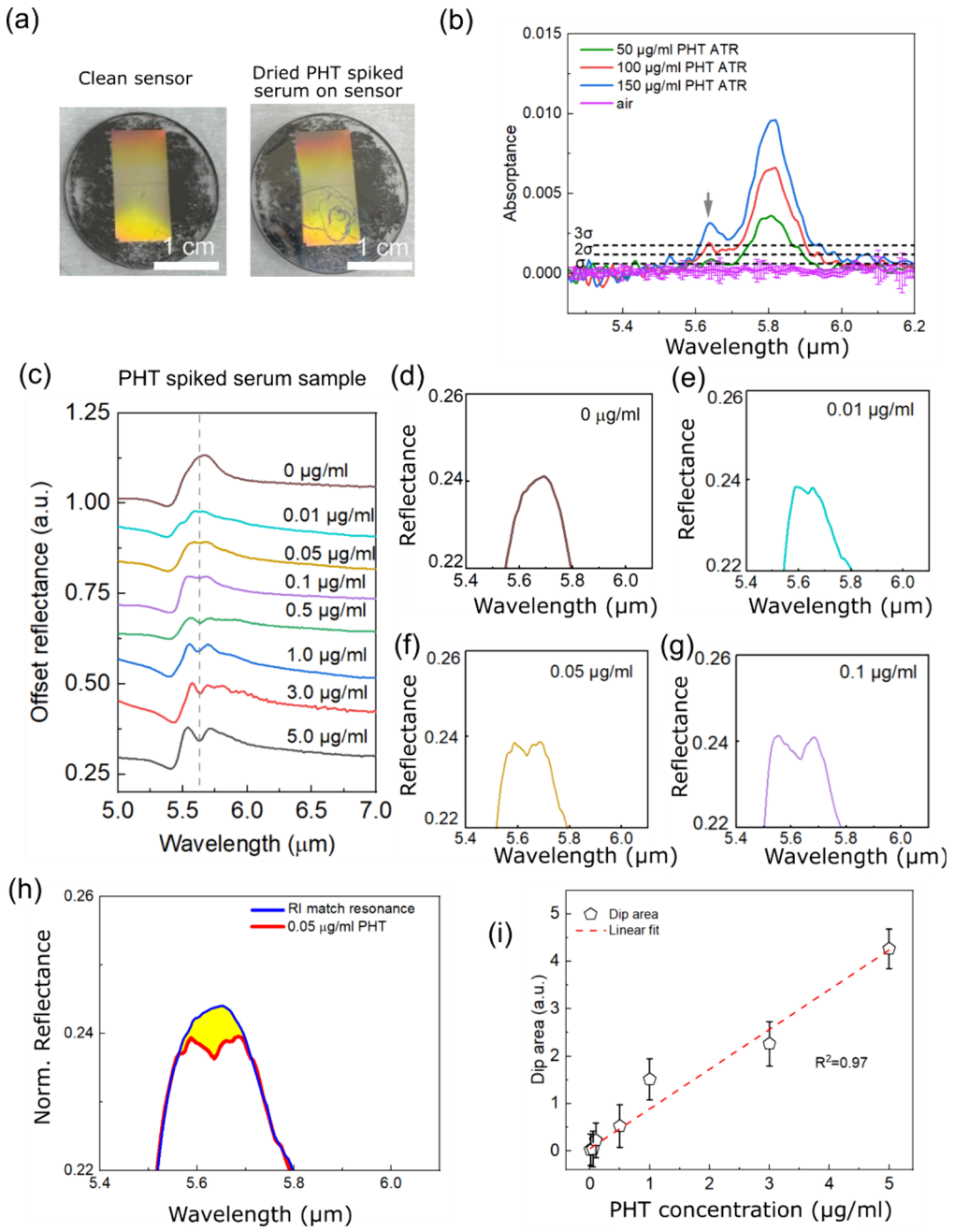


Figure 4. Measurements of PHT in spiked serum. (a) Photographs of the metasurface with and without dried PHT spots. (b) Absorption spectrum of PHT-serum solution dried on an ATR sensor surface. The absorption peak at 5.62 μm is the TDM target peak, indicated by a gray arrow. Blank references are taken as the background spectra, shown with a purple curve with error bars indicating the deviation (σ) at each wavelength, and the black dashed lines representing σ, 2σ, and 3σ at 5.62 μm. The LoD of ATR is determined to be 100 μg/ml from the 3σ value. (c) Reflection spectrum obtained using the metasurface-enhanced FTIR approach with 0.01–5 μg/mL PHT-serum solution (300 μl dried onto the metasurface). The gray dashed line marks the target PHT absorption line. (d–g) Zoomed-in views of the enhanced absorption area for each specific concentration. (h) Definition of the dip area used for quantification of absorbance enhancement. (i) Sensor response versus concentration to determine the LoD). Each concentration was washed and dried 4 times, with 10 different scans on each cycle. Samples were carefully checked by photographs, micrographs, and FTIR spectra to confirm clean washing with no crystallized PHT residues (see Figure S9, Supporting Information). Note, the limit of quantitation (LoQ) is defined by 10 times the sigma divided by sensitivity. In our case, the LoQ is 4.6 μg/ml.

and the dried analyte, as well as the angular tolerance that is compatible with an FTIR instrument. As a result, we report an advanced infrared molecular sensing platform and establish a viable framework for translating TDM to point-of-care settings. Despite these advancements, current analytical throughput is limited by multistage serum pretreatment, stringent dehydration protocols, and rigorous sample volume constraints, specifically regarding ATR overflow and large-volume drying kinetics on the metasurface. To overcome these bottlenecks, the integration of a monolithic microfluidic device for

Downloaded from pubs.acs.org/acsejf/article-pdf/11/9/8387/6739358/se-2026-022393.pdf by guest on 04 November 2026

https://doi.org/10.1021/acssensors.6c02239
ACS Sens. 2026, 11, 8387−8394

automated sample handling is required. Such an integrated architecture would bridge the gap between benchtop characterization and bedside clinical diagnostics, enabling seamless TDM migration from the laboratory to the patient.

Metasurface-enhanced FTIR (meta-FTIR) spectroscopy offers significant advantages over conventional methods, such as LCMS in speed, cost, and portability. Meta-FTIR requires a scanning time of less than 1 min and can be performed on site, eliminating delays associated with sample transport and laboratory processing, whereas LCMS typically requires more than 10 min per measurement and total turnaround times can extend to several days in clinical workflows. Although meta-FTIR sample preparation takes 10–15 min compared with 5 min for LCMS, this difference is outweighed by the elimination of delays and the need for centralized laboratory infrastructure. In addition, meta-FTIR has a low instrumentation and running cost; it does not require a laser source, and it can be miniaturized, enabling a compact, user-friendly point-of-care platform suitable for bedside or field deployment. By performing well below the clinical concentration range, our method leaves room for practical limitations such as the lack of nitrogen purging, which increases the background noise, or the drug loss during sample preparation. Regarding the latter, the filtration procedure typically results in a 30% drug loss,[19] which can be clearly accounted for.

The main source of the variance between measurements that limits more accurate quantification is the uneven distribution of phenytoin across the sample after drying rather than intrinsic sensor heterogeneity. Recent work by Miller et al. utilizing CMOS-compatible deep-ultraviolet (DUV) lithography reported a resonance wavelength variation of less than 3.7% across 322 sensors.[21] This benchmark suggests that device-to-device variability is negligible relative to sample morphology; consequently, the current sensing architecture is robust enough for quantitative accuracy within this proof-of-concept framework. Future work will focus on improving the homogeneity of the dried film by incorporating a sample well on the sensor surface to confine the evaporation area of the serum sample and ensure that it dries within a defined region. Complementary strategies, such as hydrophilic surface patterning to guide fluid distribution and controlled-humidity drying to suppress coffee-ring effects, could further improve reproducibility of the dried analyte film. Another issue is the sample preparation protocol, which currently consists of three manual steps; we are working on an integrated microfluidic device that simplifies this process into a single step and can be used by untrained personnel. These improvements will enhance the clinical applicability of metasurface-enhanced FTIR spectroscopy and move the technique even closer toward real-world therapeutic drug monitoring.

METHODS

Numerical simulations of the proposed metasurface were carried out using the finite-difference time-domain (FDTD) software package Lumerical, while rigorous coupled-wave analysis (RCWA) was employed to model the response under Gaussian beam illumination.

For fabrication, a 400 nm germanium film was deposited onto a CaF_2 wafer by plasma-enhanced chemical vapor deposition (PECVD) at the University of Southampton. The metasurface pattern was defined using electron-beam lithography (EBL) using a RAITH Voyager and AR-P 6200.18 resist (Allresist GmbH). To mitigate charging effects, a conductive AR-PC layer (Allresist GmbH) was spin-coated on top of the resist. Following exposure, the AR-PC layer was removed in deionized water, and the sample was developed in xylene for 2 min, followed by rinsing in 2-propanol isopropyl (IPA). Reactive ion etching (RIE) was then used to transfer the pattern into the germanium layer using a CHF_3:SF_6 gas mixture (14.5:12.5 sccm). The remaining resist was stripped with remover 1165 (MicroResist GmbH).

Subsequently, a 20 nm-thick Al_2O_3 coating was conformally deposited on the Ge metasurface using atomic layer deposition (ALD) (Picosun Instr.) at 300 °C, with trimethylaluminum (TMA) and H_2O as precursors. The coated sample could survive 5 min of Piranha wash without degradation of its resonance position, indicating good chemical protection. Details are shown in Figure S8, Section 8 in Supporting Information.

Measurements were performed using a commercial FTIR spectrometer (Bruker Vertex 70), configured as shown in Figure 3a with a customized perpendicular reflection setup (inset). The schematic optical layout of this setup is illustrated in Figure 3b. The customized configuration includes a one-inch-diameter beam splitter (BSW510, Thorlabs), three gold mirrors, an x–y translational mount (XYF2/M, Thorlabs), and a 3D-printed sample holder (inset of Figure 3a). Mid-infrared light generated by the FTIR thermal source enters through the right-hand chamber window, is reflected by the gold mirrors, passes through the beam splitter, and is incident on the metasurface, which is coated with dried drug molecules. The enhanced absorption signal is encoded in the reflected spectrum, which then passes back through the same beam splitter, is directed toward the left chamber window of the FTIR, and finally detected by a deuterated L-alanine doped triglycine sulphate (DLaTGS) detector at room temperature.

The ATR measurement was employed with the unit from MIRacle with three-bounce reflection ATR plates made of ZnSe, PIKE Technologies, and the unit was inserted into the FTIR spectrometer (Bruker Vertex 70). To evaluate the LoD of the ATR configuration, ten reference measurements were acquired in compressed air without any sample. Each spectrum was background-corrected to minimize systematic errors. The amplitude variations (standard deviations σ) at each wavelength were then calculated.

In order to calculate the dip area on the reflected resonance, the reference profile was derived from the reflection spectrum of the 0% PHT sample (pure ethyl acetate) and subsequently shifted to match the envelope of each absorption spectrum, thereby compensating for refractive index variations. This correction is necessary because the resonance position of the dielectric metasurface depends on the refractive index of the coating layer; as the PHT concentration changes, the effective refractive index varies, resulting in a resonance shift.

Phenytoin (Sigma-Aldrich) was dissolved in ethyl acetate (Sigma-Aldrich), and 500 μl of the solution was dried on the metasurface in a fume hood within 6 min.

Phenytoin was spiked in preprocessed serum samples; the protocol for preprocessing the serum is a three-step process. First, we employ a liquid–liquid extraction with ethyl acetate solution to remove serum proteins and water. Second, a combination of magnesium chloride and dextran sulfate sodium has been utilized to remove serum lipids. Third, we use saturated ammonium sulfate to precipitate the albumin following lipid removal. Finally, the phenytoin is spiked into the processed serum samples.

ASSOCIATED CONTENT

Supporting Information

The Supporting Information is available free of charge at https://pubs.acs.org/doi/10.1021/acssensors.6c02239.

Reflection spectrum of Ge/CaF_2 substrate; optimization of the metasurface; absorption spectrum of PHT and serum; dried spot SEM of PHT on flat Ge surface; PHT solution overflowing the ATR sensing area; sample holder and mid-IR beam scanning on the sample;

Downloaded from pubs.acs.org/ascefj/article-pdf/11/9/8387/6739358/se-2026-022393.pdf by guest on 04 November 2026

https://doi.org/10.1021/acssensors.6c02239
ACS Sens. 2026, 11, 8387−8394

reflection spectrum of dried PHT on flat Ge/CaF_2 substrate; atomic layer deposition (ALD) for reusable measurement; photos of the sample before, dried, and wash cycle of PHT, and FTIR spectrum of before, dried, and wash of PHT crystal; dip area with different incident angles; and comparison to other surface-enhanced mid-IR studies (DOCX)

AUTHOR INFORMATION

Corresponding Authors

Kezheng Li – *School of Physics, Engineering and Technology, University of York, York YO10 5DD, U.K.;* orcid.org/0000-0002-9234-3312; Email: kezheng.li@york.ac.uk

Yue Wang – *School of Physics, Engineering and Technology, University of York, York YO10 5DD, U.K.;* orcid.org/0000-0002-2482-005X; Email: yue.wang@york.ac.uk

Authors

Pin Dong – *School of Physics, Engineering and Technology, University of York, York YO10 5DD, U.K.;* orcid.org/0000-0003-0102-236X

Aneesh Vincent Veluthandath – *Optoelectronics Research Centre, University of Southampton, Southampton SO17 1BJ, U.K.;* orcid.org/0000-0003-4306-6723

Soheila Kharratian – *School of Physics, Engineering and Technology, University of York, York YO10 5DD, U.K.*

Augusto Martins – *School of Physics, Engineering and Technology, University of York, York YO10 5DD, U.K.*

Ganapathy Senthil Murugan – *Optoelectronics Research Centre, University of Southampton, Southampton SO17 1BJ, U.K.;* orcid.org/0000-0002-2733-3273

Thomas F. Krauss – *School of Physics, Engineering and Technology, University of York, York YO10 5DD, U.K.;* orcid.org/0000-0003-4367-6601

Complete contact information is available at: https://pubs.acs.org/doi/10.1021/acssensors.6c02239

Notes

The authors declare no competing financial interest.

ACKNOWLEDGMENTS

The authors thank the support of the EPSRC MISSION Programme Grant (EP/V047663/1).

REFERENCES

(1) Ates, H. C.; Roberts, J. A.; Lipman, J.; Cass, A. E. G.; Urban, G. A.; Dincer, C. On-Site Therapeutic Drug Monitoring. *Trends Biotechnol.* **2020**, *38* (11), 1262–1277.

(2) Salman, B.; Al-Khabori, M. Applications and challenges in therapeutic drug monitoring of cancer treatment: A review. *J. Oncol. Pharm. Pract.* **2021**, *27* (3), 693–701.

(3) Adaway, J. E.; Keevil, B. G. Therapeutic drug monitoring and LC-MS/MS. *J. Chromatogr. B: Anal. Technol. Biomed. Life Sci.* **2012**, *883–884*, 33–49.

(4) Carrara, S.; Widmer, N.; Rodino, F.; Du, L.; Briki, M.; Decosterd, L. A.; Marzolini, C.; Buclin, T.; Thoma, Y.; Guidi, M. Therapeutic Drug Monitoring and Point-of-Care Technologies: Opportunities and Current Challenges. *Ther. Drug Monit.* **2025**, *48*, 42.

(5) Alvau, M. D.; Tartaggia, S.; Meneghello, A.; Casetta, B.; Calia, G.; Serra, P. A.; Polo, F.; Toffoli, G. Enzyme-Based Electrochemical Biosensor for Therapeutic Drug Monitoring of Anticancer Drug Irinotecan. *Anal. Chem.* **2018**, *90* (10), 6012–6019.

(6) Mendelsohn, R.; Mao, G. R.; Flach, C. R. Infrared reflection-absorption spectroscopy: Principles and applications to lipid-protein interaction in Langmuir films. *BBA-Biomembranes* **2010**, *1798* (4), 788–800.

(7) John-Herpin, A.; Tittl, A.; Kühner, L.; Richter, F.; Huang, S. H.; Shvets, G.; Oh, S. H.; Altug, H. Metasurface-Enhanced Infrared Spectroscopy: An Abundance of Materials and Functionalities. *Adv. Mater.* **2023**, *35* (34).

(8) Neubrech, F.; Huck, C.; Weber, K.; Pucci, A.; Giessen, H. Surface-Enhanced Infrared Spectroscopy Using Resonant Nanoantennas. *Chem. Rev.* **2017**, *117* (7), 5110–5145.

(9) Adato, R.; Altug, H. In-situ ultra-sensitive infrared absorption spectroscopy of biomolecule interactions in real time with plasmonic nanoantennas *Nat. Commun.* **2013**, *4*, 2154.

(10) Leitis, A.; Tittl, A.; Liu, M. K.; Lee, B. H.; Gu, M. B.; Kivshar, Y. S.; Altug, H. Angle-multiplexed all-dielectric metasurfaces for broadband molecular fingerprint retrieval. *Sci. Adv.* **2019**, *5* (5), 2871.

(11) Kharratian, S.; Conteduca, D.; Procacci, B.; Shaw, D. J.; Hunt, N. T.; Krauss, T. F. Metasurface-enhanced mid-infrared spectroscopy in the liquid phase. *Chem. Sci.* **2022**, *13* (43), 12858–12864.

(12) Rosas, S.; Adi, W.; Beisenova, A.; Biswas, S. K.; Kuruoglu, F.; Mei, H. Y.; Kats, M. A.; Czaplewski, D. A.; Kivshar, Y. S.; Yesilkoy, F. Enhanced biochemical sensing with high-Q transmission resonances in free-standing membrane metasurfaces. *Optica* **2025**, *12* (2), 178–189.

(13) Bunaciu, A. A.; Aboul-Enein, H. Y.; Fleschin, S. Application of Fourier Transform Infrared Spectrophotometry in Pharmaceutical Drugs Analysis. *Appl Spectrosc Rev* **2010**, *45* (3), 206–219.

(14) Barretto, C. T.; Nascimento, M. H. C.; Brun, B. F.; da Silva, T. B.; Dias, P. A. C.; Silva, C. A. B.; Singh, M. N.; Martin, F. L.; Filgueiras, P. R.; Romao, W.; et al. Infrared spectroscopy as a new approach for early fabry disease screening: a pilot study *Orphanet. J. Rare Dis.* **2024**, *19* (1), 373.

(15) Chen, X. E.; Zhang, Y.; Cai, G. X.; Zhuo, J. L.; Lai, K. Z.; Ye, L. F. All-dielectric metasurfaces with high Q-factor Fano resonances enabling multi-scenario sensing. *Nanophotonics-Berlin* **2022**, *11* (20), 4537–4549.

(16) Biswas, S. K.; Adi, W.; Beisenova, A.; Rosas, S.; Arvelo, E. R.; Yesilkoy, F. From weak to strong coupling: quasi-BIC metasurfaces for mid-infrared light-matter interactions. *Nanophotonics-Berlin* **2024**, *13* (16), 2937–2949.

(17) Conteduca, D.; Arruda, G. S.; Barth, I.; Wang, Y.; Krauss, T. F.; Martins, E. R. Beyond Q: The Importance of the Resonance Amplitude for Photonic Sensors. *ACS Photonics* **2022**, *9* (5), 1757–1763.

(18) Tittl, A.; Leitis, A.; Liu, M. K.; Yesilkoy, F.; Choi, D. Y.; Neshev, D. N.; Kivshar, Y. S.; Altug, H. Imaging-based molecular barcoding with pixelated dielectric metasurfaces. *Science* **2018**, *360* (6393), 1105.

(19) Dong, P.; Li, K. Z.; Rowe, D. J.; Krauss, T. F.; Wang, Y. Protocol for Therapeutic Drug Monitoring Within the Clinical Range Using Mid-infrared Spectroscopy. *Anal. Chem.* **2024**, *96* (48), 19021–19028.

(20) Lee, W. W. Y.; McCoy, C. P.; Donnelly, R. F.; Bell, S. E. J. Swellable polymer films containing Au nanoparticles for point-of-care therapeutic drug monitoring using surface-enhanced Raman spectroscopy. *Anal. Chim. Acta* **2017**, *912*, 111–116.

(21) Miller, L. M.; Reardon, C. P.; Leslie, K.; Silver, C. D.; Male, J. S.; Mahon, C. S.; Krauss, T. F.; Johnson, S. Multiplexed Nanophotonic Sensor Arrays for Time-Resolved Biomolecular Analysis. *Biosens. Bioelectron.* **2026**, *305*, 118669.

(22) Leitis, A.; Heßler, A.; Wahl, S.; Wuttig, M.; Taubner, T.; Tittl, A.; Altug, H. All-Dielectric Programmable Huygens' Metasurfaces. *Adv. Funct. Mater.* **2020**, *30*, 1910259.

(23) Altug, H.; Oh, S.-H.; Maier, S. A.; Homola, J. Advances and Applications of Nanophotonic Biosensors. *Nat. Nanotechnol.* **2022**, *17*, 5–16.

(24) Liu, Y.; Li, J.; Xiao, S.; Liu, Y.; Bai, M.; Gong, L.; Zhao, J.; Chen, D. Revolutionizing Precision Medicine: Exploring Wearable Sensors for

Downloaded from pubs.acs.org/asceff/article-pdf/11/9/8387/6739458/se-2026-022393.pdf by guest on 04 November 2026

Therapeutic Drug Monitoring and Personalized Therapy. *Biosensors* **2023**, *13*, 726.

(25) Patsalos, P. N.; Berry, D. J.; Bourgeois, B. F. D.; Cloyd, J. C.; Glauser, T. A.; Johannessen, S. I.; Leppik, I. E.; Tomson, T.; Perucca, E. Antiepileptic Drugs—Best Practice Guidelines for Therapeutic Drug Monitoring: A Position Paper by the Subcommission on Therapeutic Drug Monitoring, ILAE Commission on Therapeutic Strategies. *Epilepsia* **2008**, *49* (7), 1239–1276.

(26) Patsalos, P. N.; Spencer, E. P.; Berry, D. J. Therapeutic Drug Monitoring of Antiepileptic Drugs in Epilepsy: A 2018 Update. *Ther. Drug Monit.* **2018**, *40* (5), 526–548.

(27) Rambeck, B.; May, T. W.; Jürgens, M. U.; Blankenhorn, V.; Jürges, U.; Korn-Merker, E.; Sälke-Kellermann, A. Comparison of Phenytoin and Carbamazepine Serum Concentrations Measured by High-Performance Liquid Chromatography, the Standard TDx Assay, the Enzyme Multiplied Immunoassay Technique, and a New Patient-Side Immunoassay Cartridge System. *Ther. Drug Monit.* **1994**, *16* (6), 608–612.

(28) Sanavio, B.; Krol, S. On the Slow Diffusion of Point-of-Care Systems in Therapeutic Drug Monitoring. *Front. Bioeng. Biotechnol.* **2015**, *3*, 20.

Downloaded from pubs.acs.org/ascefj/article-pdf/11/9/8387/6739358/se-2026-022393.pdf by guest on 04 November 2026

https://doi.org/10.1021/acssensors.6c02239
ACS Sens. 2026, 11, 8387−8394